OPEN ACCESS

GAVIN PUBLISHERS

Cardiology Research and Cardiovascular Medicine

Sun G, et al. Cardiolog Res Cardiovasc Med 3: CRCM-133.

Research Article

DOI: 10.29011/2575-7083. 000033

Zucker Diabetic Sprague Dawley (ZDSD) Rat, A Spontaneously Diabetic Rat Model Develops Cardiac Dysfunction and Compromised Cardiac Reserve

Gao Sun*, Guodong Zhang, Charles V. Jackson, Yi-Xin (Jim) Wang

Cardiovascular and Metabolic Diseases Research, Crown Bioscience Inc, China

***Corresponding author:** Gao Sun, Cardiovascular and Metabolic Diseases Division, Crown Bioscience Inc., 6 Beijing West Road, Science & Technology Park, Taicang Economic Development Area, Jiangsu Province, 215400, P.R. China. Tel: +8613862278837; +8651253879828; Email: gao.sun@crownbio.com

Citation: Sun G, Zhang G, Jackson CV, Wang YXJ, (2018) Zucker Diabetic Sprague Dawley (ZDSD) Rat, A Spontaneously Diabetic Rat Model Develops Cardiac Dysfunction and Compromised Cardiac Reserve. Cardiolog Res Cardiovasc Med 3: 133. DOI: 10.29011/2575-7083.000033

Received Date: 31 May, 2018; **Accepted Date:** 13 June, 2018; **Published Date:** 22 June, 2018

Abstract

Introduction: Diabetic Cardiomyopathy (DC) is the leading cause of morbidity and mortality among all complications of Type 2 Diabetes (T2D) and obese patients. It is characterized by an initial cardiac hypertrophy followed by declines in cardiac functions, which ultimately leads to heart failure. No rodent models fully captured phenotypes of DC. The Zucker Diabetic Sprague Dawley (ZDSD) rat, a new generation of T2D rat model with intact leptin signaling features with slow onset of diabetes, obesity and dyslipidemia, which closely mimics the development of the disease in patients. Here we sought to evaluate the cardiac function during the development of metabolic syndromes in ZDSD rats.

Methods: Age matched male ZDSD and SD rats were monitored for blood pressure and cardiac function using Echocardiography. Animals were also challenged with 1 mg/kg dobutamine for the assessment of cardiac reserve.

Results: ZDSD rats developed hypertension from age of 18 weeks with both systolic and diastolic blood pressure significantly higher than controls. Their Left Ventricular (LV) functions were compromised along with changes in cardiac morphology. At resting state, ZDSD rats showed thickening of LV posterior wall from age of 18 to 22 weeks after which cardiac walls became thinner with larger LV cavity volume. Both Ejection Fraction (EF) and transmitral E/A ratio of LV declined at 34 weeks old. Upon treatment with dobutamine, ZDSD rats had much lower EF and Fractional Shorterning (FS) compared to SD rats, suggesting the loss of contractility and cardiac reserve of the animals.

Conclusion: ZDSD rats which carry multiple dysmetabolic phenotypes are spontaneously hypertensive with reduction in LV function and cardiac reserve which resembles ultrasonic symptoms of diabetic cardiomyopathy patients. Therefore, ZDSD rats may serve as a suitable preclinical model to study potential therapeutic approaches to treat cardiomyopathy with presence of metabolic syndromes.

Keywords: Cardiomyopathy; Diabetes; Echocardiography; Obesity; Ultrasound

Abbreviations

AGE	:	Advanced Glycated End-Product
BNP	:	B-Type Natriuretic Peptide
CO	:	Cardiac Output
DC	:	Diabetic Cardiomyopathy
E/A ratio	:	Ratio of The Peak Trans-Mitrol Flow Velocities at Early (E) And Late (A) Diastole
ECG	:	Electrocardiography
EDV	:	Left Ventricular End Diastolic Volume
EF	:	Ejection Fraction
ER	:	Endoplasmic Reticulum
ESV	:	Left Ventricular End Systolic Volume

FS	:	Fractional Shorterning
HR	:	Heart Rate
LVID	:	Left Ventricular Inner Diameter
LVPW	:	Left Ventricular Posterior Wall
LV	:	Left Ventricle
PWV	:	Pulse Wave Velocity
SD	:	Sprague Dawley
SV	:	Stroke Volume
T2D	:	Type 2 Diabetes
ZDF	:	Zucker Diabetic Fatty
ZDSD	:	Zucker Diabetic Sprague Dawley

Introduction

Cardiovascular dysfunction is the leading cause of morbidity and mortality among all complications of type 2 diabetes and obesity patients. The risk of heart failure significantly increases in patients with type 2 diabetes [1]. With the prevalence of diabetes, the number of patients with diabetic cardiomyopathy also surged in the past decade. Using Echocardiography, the morphological and functional changes of cardiac ventricles during the development of diabetic cardiomyopathy can be monitored longitudinally [2,3]. At the early stage of the disease, cardiac hypertrophy is prominent with increased Left Ventricular (LV) mass and wall thickness. As the disease progresses, diastolic function of the heart compromises, which is characterized by the reduction in ratio of early to late (E/A) transmitral flow velocities. The phenomenon is followed by declines in systolic function at the late stage, which is manifested by reductions in percentages of Ejection Fraction (EF) and Fractional Shortening (FS) of the LV. Accompanying the systolic functional changes, LV experiences enlargement in inner cardiac dimension and thinning of the cardiac wall [2,4,5]. Eventually, heart failure may ensue as a direct consequence of the loss of the cardiac function [3].

Although the exact cause of diabetic cardiomyopathy is not fully understood, many risk factors and molecular mechanisms have been proposed [6]. These include Advanced Glycated End-Product (AGE) accumulation, intramyocardial inflammatory cytokine increase, mitochondrial dysfunction, lipotoxicity, oxidative and endoplasmic reticulum (ER) stress etc. that lead to impairment of intracellular Ca^{2+} handling, fibrosis and myocardial dysfunction [17-19].

In order to facilitate the understanding of the disease mechanism, pathology and the identification of drug targets for treating diabetic cardiomyopathy, multiple type 2 diabetic rodent models have been characterized for phenotypes of cardiomyopathy [20]. *Ob/ob* and *db/db* mice develop obesity and diabetes from age of 6-8 weeks old as a result of recessive mutation of obesity gene, leptin and defects in leptin receptor respectively. Impaired diastolic function with reduced E/A ratios were noticed in *ob/ob* mice at the age of 11 weeks, while contractility of LV was mildly affected upon dobutamine stimulation at 11 weeks and reductions in EF% at resting states at 22 weeks old without changes in LV mass [21-24]. By comparison, *db/db* mice developed cardiac hypertrophy with increased LV mass and wall thickness at the age of 22 weeks [24]. Concomitantly, the animals have shown diastolic and systolic dysfunction in LV with significant reductions in E/A ratios and EF% at age of 12 and 22 weeks respectively [24,25]. In diabetic rat models, Zucker Diabetic Fatty (ZDF) rats developed impaired diastolic function with reduction in E/A ratio at age of 30 weeks [26]. This was accompanied by increases in Inter Ventricular (IV) septal wall thickness and decreases in LV dimension. At 44 weeks, reduction in End-Diastolic Volume (EDV) and LV mass without showing defects in systolic function with no impact on EF% at 44 weeks' old were noticed [27]. Therefore, ZDF rats do not fully capture the decline of systolic function in diabetic cardiomyopathy patients.

Zucker Diabetic Sprague Dawley (ZDSD) rat is a new generation of diabetic rat model with intact leptin signalling [28]. The model was generated by selective breeding ZDF rats and obese-prone SD rats followed by over 35 back-crossings. As a result, ZDSD rats possess multiple metabolic disorders such as diabetes, obesity and dyslipidemia etc. with phenotypes highly close to T2D patients [28]. Thus, these animals have distinctive pre-diabetic and diabetic stages, where glucose started to elevate at the age of 16-18 weeks [28]. Serum insulin levels displayed bi-phasic fluctuation where pre-diabetic insulin hyper-secretion was noticed between 13-18 weeks, after which insulin levels start to decline [28]. More importantly, the animals showed multiple diabetic late complications such as diabetic nephropathy [29], neuropathy and delayed wound healing, which make ZDSD rat an ideal pre-clinical model for study diabetes and related complications [30,31].

The main aim of this study is to evaluate the cardiac morphology and function in ZDSD rats during the development of diabetes using non-invasive Echocardiography and to assess the possibility of using ZDSD rats as a model for the development of therapeutic approaches for treating diabetic cardiomyopathy.

Materials and Methods

Animals

Male ZDSD (n=8) and age-matched Sprague Dawley (SD) (n=8) rats were obtained from Crown Bioscience Inc. and Envigo (Indianapolis, US) respectively. Animals were housed 2 per cage and were fed ad libitum on Purina 5008 regular rodent chow (protein: 26.8%, carbohydrate: 56.4%, fat: 16.7% in calories) and house water. Room temperature was monitored and maintained

at 20-26°C with the light cycle set at 12 hours (6:00-18:00). All procedures were approved by the Association for Assessment and Accreditation of Laboratory Animal Care (AAALAC) in Crown Bioscience Inc.

Determination of Blood Glucose

Morning and afternoon tail vein blood glucose levels from fed animals were determined using a hand-held glucometer (Stat Strip Xpress glucometer, Nova Biomedical, Waltham MA, USA). The tail of rats will be clipped from the tail end to release a drop of blood for glucometer strips reading.

Tail Cuff Blood Pressure Measurement

Blood pressure measurements were taken on conscious rats using tail cuff method by a non-invasive rat/mouse tail cuff system (CODA high throughput system, Kent Scientific, Torrington CT, USA). 15 cycles of measurement were taken and the first 5 were performed as acclimatization not counted into the final calculation.

Pulse Wave Velocity Measurement

Pulse wave velocity was measured as reported elsewhere [32]. In short, rats were anesthetized and maintained with isoflurane. The animal was situated in the supine position and ECG electrodes were attached to collect a lead II ECG signal. Sonoscope S8 expert system with a 12-14 MHz linear array transducer (L742) was used to scan the carotid and iliac arteries under colour-flow Doppler mode. For measuring diameters of carotid, M mode was employed. The total time for each study was approximately 10 minutes. PWV was calculated as: PWV=Distance (D)/Time (T), where D is the distance in cm from carotid to iliac measurement sites and T= (R to iliac foot)- (R to carotid foot) in msec. Three consecutive time differences from each measurement was averaged to obtain the average T for the PWV measurement.

Determination of Cardiac Structure and Function

Echocardiography was performed on isofluorane anesthetized rats when situated on a supine position using Sonoscope S8 expert with 12-14 MHz linear array transducer. For measuring Left Ventricular (LV) dimension (eg: LV Inner Diastolic Diameter (LVIDd), LV Inner Systolic Diameter (LVIDs), End Diastolic Volume (EDV), End Systolic Volume (ESV) and Stroke Volume (SV)), wall thickness (eg: LV posterior wall (LVPW)) and systolic function (eg: Ejection Fraction (EF), Fractional Shortening (FS)), long axis view of the heart was applied from M mode tracing. For measuring diastolic function (eg: E/A ratio), four chamber view of the heart was applied from colour Doppler mode tracing.

Dobutamine Stress Test

Rats under isoflurane anesthesia were injected intraperitoneally with dobutamine (1 mg/kg). LV structure and function were measured with echocardiography before and at 1, 5, 10, and 20 min after injection. Long axis view of the heart was applied from M mode tracing. After last time point, animals were removed from isoflurane and all animals recovered from the test. The Area Under the Curves (AUCs) of HR, EF%, FS% and ESV during the 20 min test were also calculated.

Serum Cardiac Biomarker Analysis

Serum BNP levels were determined with a rat Meso Scale Discovery kit (#K153KFD, Rockville MD, USA) from blood collected from the tail vein.

Histology

The longitudinal sections of the left ventricle of hearts collected at termination were fixed in 10% neutral buffered formalin. H&E staining and Masson's trichrome staining were processed on paraffin embedded slides. General assessment of myocyte necrosis, fibrosis and aorta thickening/plagues were performed by a board certified pathologist.

Statistical Analysis

All data were expressed as mean ± Standard Error (SE). Statistical analysis was performed using unpaired student t test or one-way or two-way ANOVA with post hoc comparison. P-values less than 0.05 were considered statistically significant.

Results

Obesity, Hyperglycemia and Hypertension with Normal Arterial Stiffness

ZDSD rats were obese and heavier than SD rats from age of 14 to 30 weeks (Figure 1A). At 34 weeks, ZDSD rats were comparable to SD in weight (Figure 1A). By contrast, ZDSD became severely hyperglycemic at age of 30 weeks with both morning and afternoon blood glucose levels approaching 400 mg/dl (Figures 1B, C). However, the age of elevation in blood glucose levels in ZDSD rats showed differences depending on the time of measurement, thus ZDSD rats started to show significant increases in morning blood glucose levels at 22 weeks, while the age for increases in afternoon levels were 4 weeks earlier (Figures 1B, C).

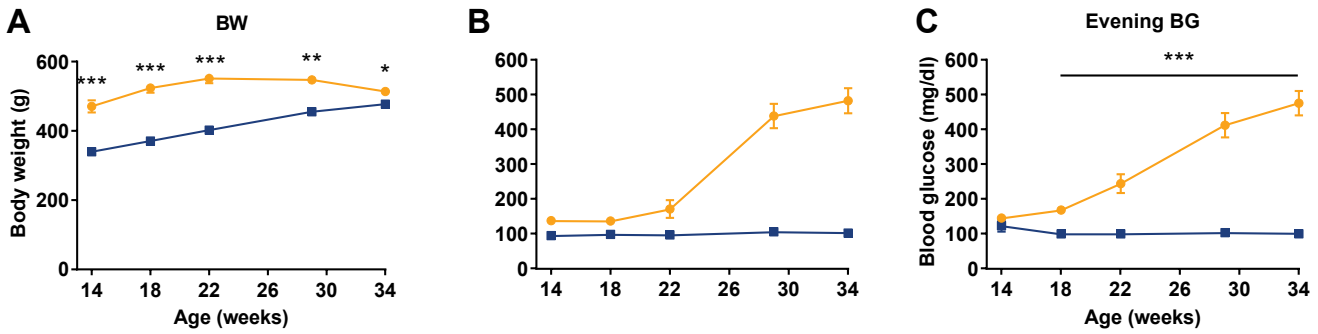

Figures 1(A-C): Spontaneously developed diabetes and obesity in ZDSD rats. **(A)** Body weight **(B)** morning (8:00) and **(C)** evening blood glucose (17:00). $^{*}p<0.05$, $^{**}p<0.01$, $^{***}p<0.001$ ZDSD vs age-matched control SD rats.

ZDSD rats were spontaneously hypertensive, with systolic blood pressure significantly higher than SD rats from age of 18 weeks while diastolic blood pressure was higher from age of 22 weeks (Figures 2A, B). However, PWV was comparable (Figure 2C) with similar systolic and diastolic carotid diameters between two groups (Figures 2D-F), suggesting that the elasticity of arterials in ZDSD rats was not compromised at the ages evaluated. The intra-observer variability co-efficiency for PWV at ages tested were between 0.08 and 0.21%.

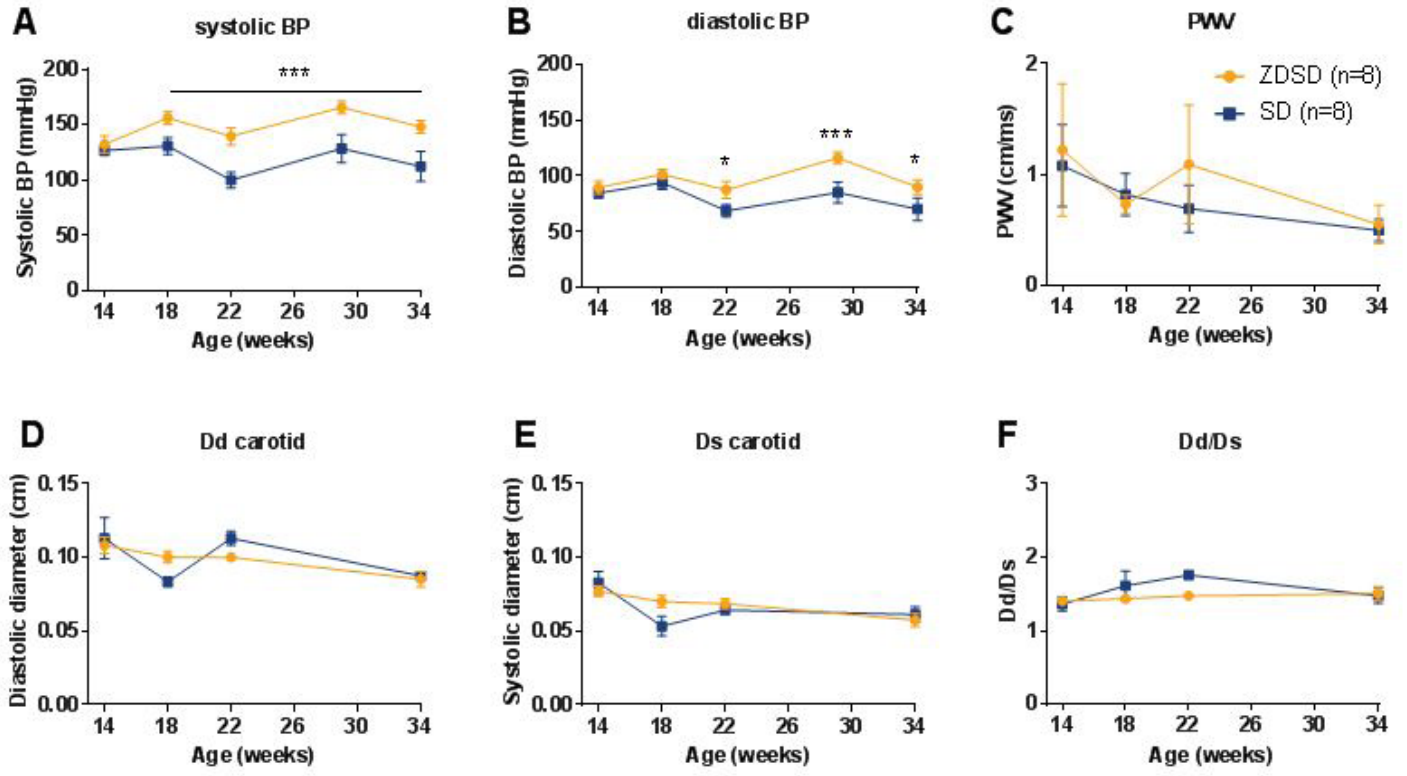

Figures 2(A-F): Spontaneously hypertensive ZDSD rats displayed normal arterial stiffness. **(A)** Systolic and **(B)** diastolic blood pressure, **(C)** pulse wave velocity, **(D)** diastolic and **(E)** systolic inner diameters and **(F)** their ratios of carotid. $^{*}p<0.05$, $^{**}p<0.01$, $^{***}p<0.001$ ZDSD vs age-matched control SD rats.

Cardiac Function and Morphology at Resting Condition

Compromised left ventricular systolic and diastolic function

The systolic function of LV of ZDSD rats also displayed bi-phasic changes with initial increases in EF% and FS% from 18-22 weeks followed by declines to baseline at 30 weeks and below SD rats at 34 weeks onwards (Figures 3A, B and Table 1). The intra-observer variability co-efficiency for EF% of ZDSD and SD rats at ages tested were between 1.1 and 2.2%, while the value for FS% were between 1.7 and 2.5%.

The diastolic function of ZDSD rats was also compromised at 34 weeks manifested by the significant reduction in E velocity and E/A ratio (Figures 3C-E).

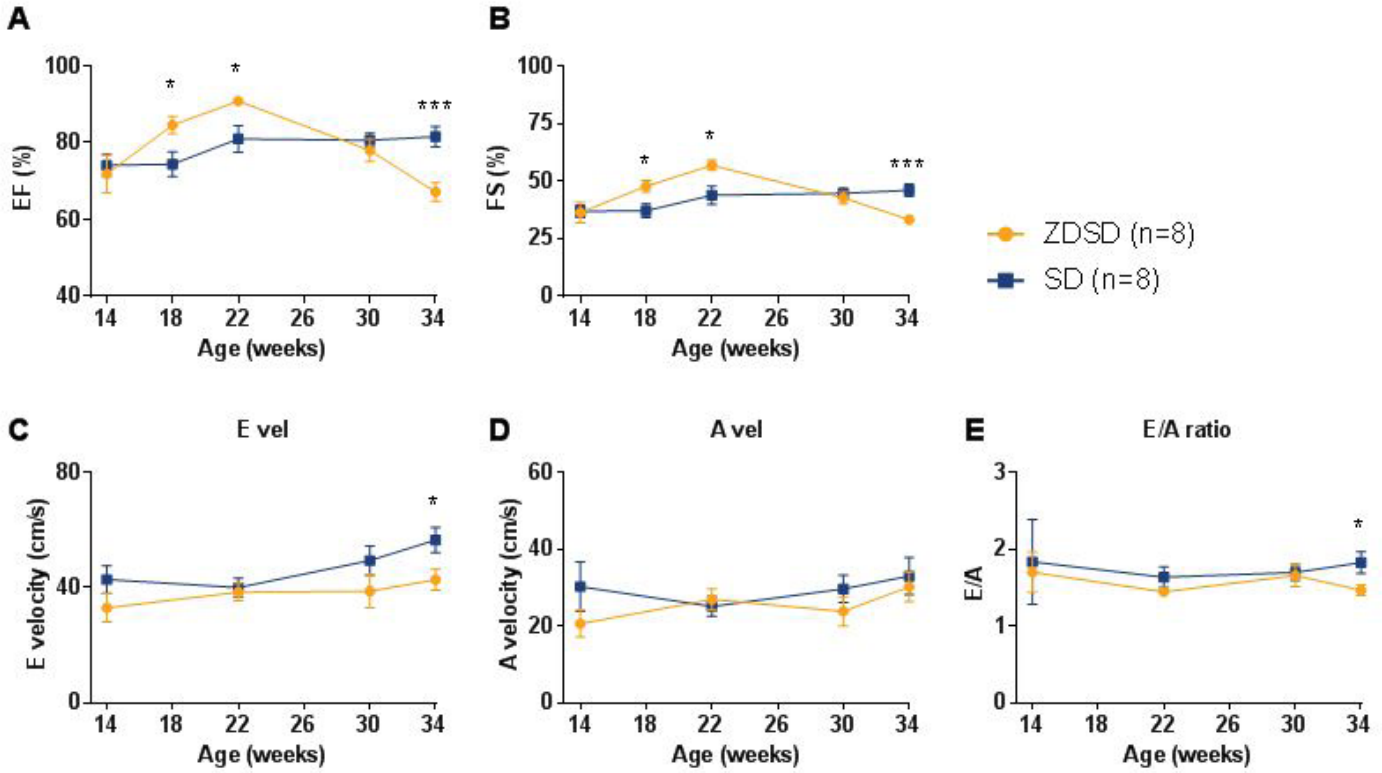

Figures 3(A-E): Cardiac dysfunction at resting condition in ZDSD rats at 34 weeks' old. Systolic dysfunction: **(A)** EF% and **(B)** FS%. Diastolic dysfunction: **(C)** early, **(D)** late trans-mitral velocity and **(E)** E/A ratio. *p<0.05 ZDSD vs age-matched control SD rats.

	SD (n=8)	ZDSD (n=8)	P value
LVPWd (cm)	0.190 ± 0.010	0.180 ± 0.007	0.468
LVPWs (cm)	0.270 ± 0.018	0.238 ± 0.012	0.181
LVIDd (cm)	0.747 ± 0.022	0.846 ± 0.023	**0.014**
LVIDs (cm)	0.400 ± 0.024	0.563 ± 0.021	**0.000**
EDV (ml)	0.934 ± 0.075	1.331 ± 0.101	**0.010**
ESV (ml)	0.173 ± 0.031	0.429 ± 0.039	**0.000**
SV (ml)	0.763 ± 0.066	0.901 ± 0.087	0.233
HR (bpm)	279.143 ± 4.954	231.285 ± 5.489	**0.000**
CO (ml/min)	212.933 ± 19.184	201.365 ± 20.038	0.664

Table 1: Left ventricular wall thickness, volume and cardiac function at resting condition in ZDSD rats and their SD controls at age of 34 weeks' old.

Biphasic changes in left ventricular inner dimension, wall thickness

The changes in heart dimension and wall thickness of ZDSD rats appeared to be biphasic compared to SD rats. After 18 weeks of age, ZDSD rats developed thicker LVPW at both the systolic and diastolic phases vs. SD rats, which became similar between the 2 groups at 30 weeks (Figure S1). At 34 weeks, both posterior wall thickness at systolic (LVPWs) and diastolic (LVPWd) states remained comparable to SD rats (Table 1). Systolic and diastolic LVID (LVIDs and LVIDd) were larger in ZDSD compared to SD rats at age of 34 weeks, while the sizes were smaller or comparable

to control SD rats respectively before 30 weeks (Table 1 and Figures S2A, B). As a result, EDV and ESV expanded in ZDSD rats at the age of 34 weeks (Table 1 and Figures S2C, D). In addition, ZDSD rats were lower in heart rate with average heart rate of 62 ± 5 bpm lower than control animals (Table 1). Stroke volume and cardiac output were not significantly different between the groups (Figures S2E, F).

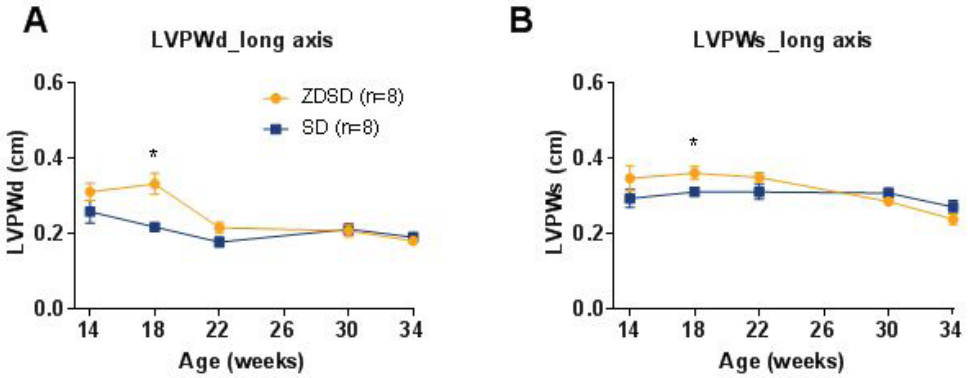

Figure S1: Biphasic changes in LV posterior wall thickness of ZDSD rats. Thickness of the left ventricular posterior wall at (A) diastole (LVPWd) and (B) systole (LVPWs). *p<0.05 ZDSD vs age-matched control SD rats.

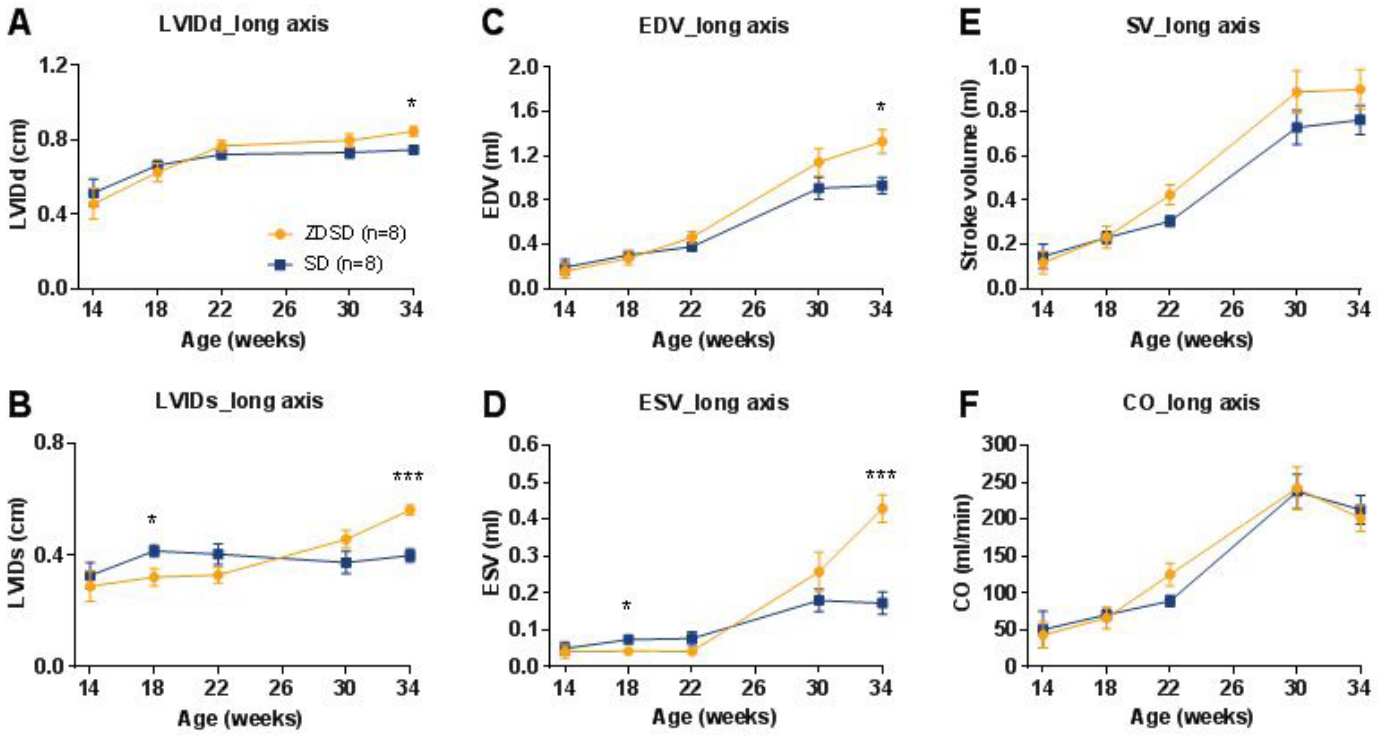

Figures S2(A-F): Biphasic changes in LV cavity volume of ZDSD rats. **(A)** Diastolic and **(B)** systolic LVID, **(C)** EDV, **(D)** ESV, **(E)** SV and **(F)** CO of the LV. *p<0.05 ZDSD vs age-matched control SD rats.

Reduced left ventricular contractility under dobutamine stress test

At 30 and 34 weeks of age, animals were challenged with 1 mg/kg dobutmaine, during which the heart dimension and systolic function were monitored. As shown in Figure 4A, intraperitoneal injection of dobutamine into SD rats led to a quick surge in heart rate (<1 min) suggesting the effectiveness of the compound. In accompany with the change, the heart contracted fully with sharp decreases in ESV (Figure 4B). As a result, the EF% and FS% in SD rats were close to 100 and 80% after dobutamine treatment (Figures 4C, D). In comparison, despite the increase of heart rate in ZDSD rats during the test, their hearts failed to contract fully, leading to a wider gap between IVS and LVPW during each contracting cycle (Figure S3E). As a result, the ESV in ZDSD rats were much higher than those in SD controls (Figure 4F), and the EF% and FS% were dramatically lower in ZDSD rats. As the LV systolic and diastolic function of ZDSD rats at resting state deteriorated, the LV contractility worsened under dobutamine stress test at 34 weeks' old (Figures S3A-D).

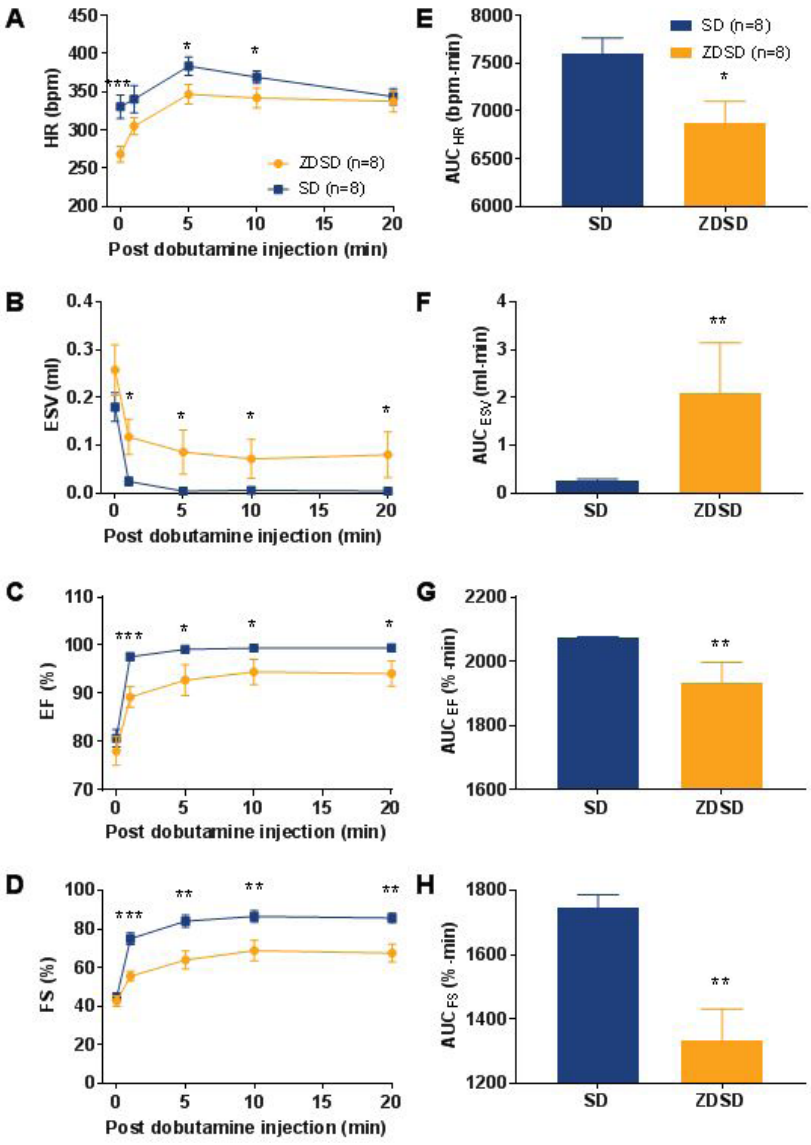

Figures 4(A-H): Reduced cardiac functional reserve measured by dobutmaine stress test in ZDSD rats at 30 weeks' old. **(A-D)** Response curve and **(E-H)** area under the curve of **(A, E)** HR, **(B, F)** ESV, (**C, G)** EF% and **(D, H)** FS% following intraperitoneally injection of 1 mg/kg dobutmine. *p<0.05, **p<0.01 ZDSD vs age-matched control SD rats.

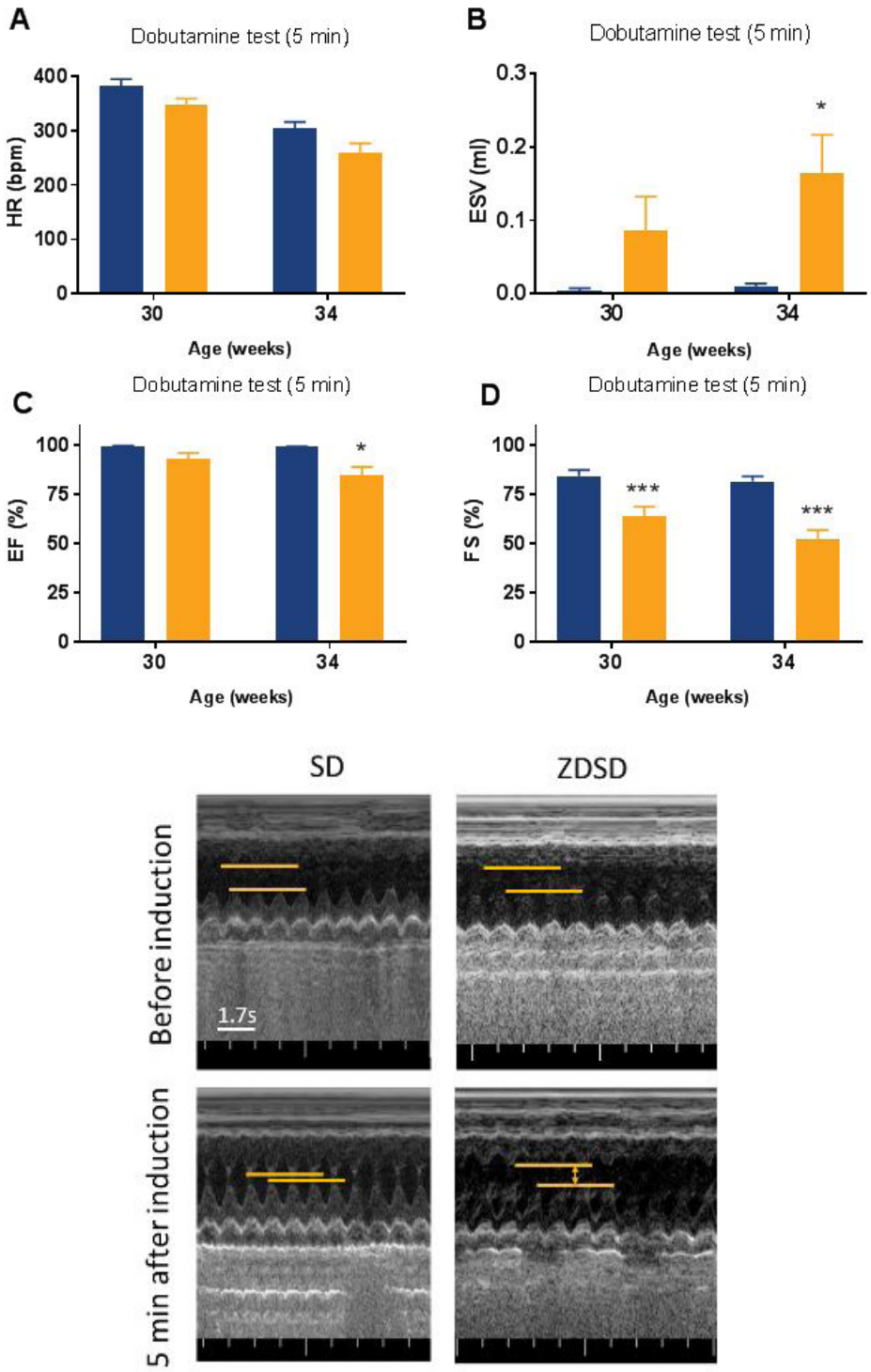

Figures S3(A-E): Compromised LV contractility of ZDSD rats at 30 and 34 weeks during dobutamine stress test. **(A)** HR, **(B)** ESV, **(C)** EF%, **(D)** FS% of ZDSD rats and their SD controls at 5 min post dobutamine administration. **(E)** Representative echocardiographic image of LV viewed at long axis under M mode in ZDSD rats at 30 weeks' old during dobutamine stress test. *p<0.05, ***p<0.001 ZDSD vs age-matched control SD rats.

ZDSD rats have unaltered BNP levels and normal histology of LV

The serum BNP levels during the development of the cardiac dysfunction of the ZDSD rats remained steady with comparable values between groups at 34 weeks old (2.84 ± 0.54 in ZDSD vs. 2.41 ± 0.54 pg/ml in SD) (Fig. S4). In addition, no significant histopathological changes were observed in the LV of animals examined (data not shown).

Discussion

ZDSD Rats Develop Baseline Diastolic and Systolic Cardiac Dysfunction with Biphasic Changes in LV Morphology

Despite the availability of multiple diabetic and obese rat models such as ZDF, GK and DIO rats on the market, their development in cardiomyopathy do not fully capture human disease progression [20]. We have demonstrated here that the new generation of type 2 diabetic rat, ZDSD with intact leptin signalling possesses the majority of the phenotypes of diabetic cardiomyopathy during its development of diabetes [28]. More importantly, the phenotypic changes in cardiac morphology and function resembles the disease progression in diabetic cardiomyopathy patients [4,5].

Similar to ZDF rats, ZDSD rats showed bradycardia from age of 30 weeks (Figure S3A), though it is not known if it is due to the similar intrinsic properties of pacemaker cells in the sinoatrial node as in ZDF [33]. However, unlike ZDF rats, ZDSD rats developed spontaneous hypertension and hyperglycemia after age of 18 and 22 weeks respectively (Figure 2) with steady increases in body weight (Figure 1), body fat and biphasic changes in plasma insulin [28]. Although the cause of hypertension is not clear as their arterial stiffness is not compromised (Figure 2C), their IVS and LVPW grew thicker at 18 weeks' old compared to 14 weeks or age-matched SD controls (Figure S1). As a result, LV ejection fraction slightly elevated probably to compensate for the hypertrophy of the LV (Figure 3A). In hypertension patients, a compensatory increase in cardiac wall thickness is usually witnessed [34]. It is possible that the initial increases in IVS and LVPW in ZDSD rats could be caused by the spontaneous hypertension of these animals. Interestingly, the initial increase in cardiac dimension started to decrease in ZDSD rats and these changes corresponded to the start of the elevation of glucose at age of 22 weeks in the animals, suggesting a possible intrinsic correlation between cardiac morphology or functional changes and the progression of diabetes from pre-diabetic state. As the hyperglycemia of the animals persisted, the morphology of the LV further developed with LVPW becoming thinner resulting in the enlargement of LV chamber with both EDV and ESV expanded compared to SD controls at week 34 (Figure S1, S2 and Table 1). Concomitantly, both diastolic and systolic functions were compromised as manifested by reduction in E/A ratio and EF (Figure 3, 4 and Table 1). The distinctive biphasic changes in cardiac morphology and function are similarly seen in human patients.

ZDSD rats have intact leptin signaling and show leptin resistance when the animals grow obese and diabetic [28]. This creates a unique advantage over traditional ZDF rat model where leptin receptor is defective [20]. It is known that leptin is involved in the cardiac contractility and LV hypertrophy [35]. Treatment of cardiomyocytes from *ob/ob* mice enhanced phosphorylation of phospholamban (PLN) which caused sarcoplasmic reticulum Ca^{2+} sequestration from the cytosol that resulted in cardiomyocyte contraction [36]. On the other hand, neutralization of LepR using antibodies alleviated cardiac hypertrophy in coronary artery ligated rats [37]. Therefore, it is likely that depletion of downstream leptin signaling in ZDF rats might have effects on the morphology and function of the heart. Although the exact impact of lack of leptin receptor in ZDF rats on manifestation of cardiac changes is not known, ZDF rats do not exhibit impairment in systolic function with unaltered EF at age of 44 weeks, whereas ZDSD rats became defective in systolic function from age of 34 weeks [27] (Figure 3). Impairments in diastolic functions were noticed in both ZDSD and ZDF rats after age of 34 and 30 weeks respectively. Morphologically, both strains developed enlarged LV inner volume after 34 weeks at systolic and diastolic states possibly to increase the cardiac preload [38]. Therefore, ZDSD rats have similar morphological changes in LV and impairment of diastolic function as ZDF rats, but with additional demonstration of decline in systolic function of the LV, which makes it more relevant to diabetic cardiomyopathy.

ZDSD Rats Have Reduced Cardiac Reserve

Impairment in systolic function normally occurs in the late stage of diabetic cardiomyopathy in patients with no appearance of the defects at earlier time points [6]. In clinical practice, dobutamine which stimulates β1 receptors of sympathetic nerve to induce full contractility of the LV is sometimes used in a dobutamine stress test to evaluate the contractility reserve and other cardiac diseases in patients when coupled with echocardiography as an early diagnostic tool [39,40]. Dobutamine stress test was also adopted in pre-clinical research for the detection of subtle changes in cardiac reserve or defects in experimental animals [41,42]. In SD rats, 1 mg/kg can allow almost full outflow of the blood from the LV shortly after the drug administration, while the levels in ZDSD rats were significantly lower from 30 weeks old (Figure 4). One month later, lowering of the LV contractility at resting state in ZDSD rats were evident (Figure 2). The results suggested that dobutamine test can be used to predict declines in baseline systolic function in ZDSD rats. Moreover, the results indicated that the progression of diabetic cardiomyopathy in ZDSD rats also has clear stages that are similar to the development of the disease clinically.

Absence of Atherosclerosis, Serum BNP Changes and Fibrosis in Hearts of ZDSD Rats

Long term obesity is usually accompanied by atherosclerosis with accumulation of lipid and immune cell-related plague in arterials [43]. The resulting blockade of blood flow in coronary artery is the leading cause for myocardial infarction and heart failure [44]. It is suggested that impact of diabetes on cardiovascular changes might start from pre-diabetic state in patients. The chronic hyperglycemia during long pre-diabetic stage might induce accumulation of reactive oxygen species and advanced glycated product, hence leading to endothelial impairment via pro-inflammatory signaling. This may pose high risk in defects in vessel relaxation and vasculature stiffness [45]. ZDSD rats have extended pre-diabetic phase without diet induction and were defective in vascular relaxation in response to acetylcholine when fed with high fat diet [30]. Therefore, an impairment in vascular stiffness and function might be noticed in ZDSD rats. However, it is rather uncommon to see the development of stiffness in arterials in rodents due to high levels of anti-atherosclerotic HDL, unless high fat diet with animals pre-disposed to atherosclerosis such as ApoE/LDLR KO mice were used [46]. Similarly, we were not able to observe the changes in arterial stiffness in ZDSD rats with comparable PWV and carotid diameters between the groups (Figure 2C). Although ZDSD rats have longer pre-diabetic state than other diabetic rodent models, the relatively short period of this state compared to human patients and the stronger capability of maintaining elasticity of vasculature in rodents is not enough to induce visible changes in vasculature. We were also not able to detect the differences in serum BNP which are indicators for heart failure (Figure S4), during which the levels would normally rise. It is suggested that the ZDSD rats, though had declined systolic function did not reach the state where heart failure might occur. Concomitantly no fibrosis was seen in the heart of ZDSD rats at 34 weeks old, as compared to ZDF rats which saw fibrosis in LV at 19 weeks old [47]. However, ZDF rats develop severe diabetes faster than ZDSD rats. It is likely that the prolonged hyperglycemic state can accelerate the formation of fibrotic tissues in heart.

Limitations

Despite that ZDSD rats have shown clinically relevant phenotypes in cardiomyopathy with declines in systolic function, there are still some limitations of the model in the pre-clinical use. The late onset of LV systolic function (>34 weeks) will certainly create operational cost for the holding facilities. In addition, the lack of fibrosis and BNP changes in ZDSD rats at 34 weeks old, suggesting that an extended development period might be needed for the animal to develop hear failure, hence to be used for late stage cardiac dysfunction studies. On the other hand, the study was conducted mainly in male animals, as male ZDSD rats have higher incidence of developing hyperglycemia than females [28]. The usage of female animals will be limited.

Conclusion

Here we have evaluated and shown that spontaneously obese and diabetic ZDSD rats with intact leptin signaling can develop multiple changes in cardiac morphology with impairment in diastolic and systolic function of the LV that are similar to diabetic cardiomyopathy patients. Therefore, ZDSD rats might serve as a suitable pre-clinical model for the research of diabetic cardiomyopathy.

Acknowledgements

The authors gratefully acknowledge the excellent technical assistance of Anita Tepool, Coy, K, Lawson J, Bass M, Brown K and other vivarium staffs for their technical support and professional caring of the animals in the experiments.

Conflict of Interest

No conflict of interest declared.

Author Contributions Statement

GS took charge of the study design, experiment performing, data analysis, result interpretation and manuscript writing, had full access to all the data in the study and are responsible for the integrity and accuracy of the experimental procedures. GZ performed experiments, data analysis and discussion. CJ and YW were involved in the study discussion. All authors read and approved the final manuscript for submission.

References

1. Selvin E, Lazo M, Chen Y, Shen L, Rubin J, et al. (2014) Diabetes mellitus, prediabetes, and incidence of subclinical myocardial damage. Circulation 130: 1374-1382.
2. Houser SR, Margulies KB, Murphy AM, Spinale FG, Francis GS, et al. (2012) Animal models of heart failure: a scientific statement from the American Heart Association. Circ Res 111: 131-150.
3. King M, Kingery J, Casey B (2012) Diagnosis and evaluation of heart failure. Am Fam Physician 85: 1161-1168.
4. Boyer JK, Thanigaraj S, Schechtman KB, Perez JE (2004) Prevalence of ventricular diastolic dysfunction in asymptomatic, normotensive patients with diabetes mellitus. Am J Cardiol 93: 870-875.
5. Fang ZY, Schull-Meade R, Leano R, Mottram PM, Prins JB, et al. (2005) Screening for heart disease in diabetic subjects. Am Heart J 149: 349-354.
6. Bugger H, Abel ED (2014) Molecular mechanisms of diabetic cardiomyopathy. Diabetologia 57: 660-671.
7. Ma H, Li SY, Xu P, Bapcock SA, Dolence EK, et al. (2009) Advanced glycation end product (AGE) accumulation and AGE receptor (RAGE) up-regulation contribute to the onset of diabetic cardiomyopathy. J Cell Mol Med 13: 1751-1764.

8. Westermann D, Van Linthout S, Dhayat S, Dhayat N, Escher F, et al. (2007) Cardioprotective and anti-inflammatory effects of interleukin converting enzyme inhibition in experimental diabetic cardiomyopathy. Diabetes 56: 1834-1841.

9. Westermann D, Van Linthout S, Dhayat S, Dhayat N, Schmidt A, et al. (2007) Tumor necrosis factor-alpha antagonism protects from myocardial inflammation and fibrosis in experimental diabetic cardiomyopathy. Basic Res Cardiol 102: 500-507.

10. Konig A, Bode C, Bugger H (2012) Diabetes mellitus and myocardial mitochondrial dysfunction: bench to bedside. Heart Fail Clin 8: 551-561.

11. Lee Y, Naseem RH, Park BH, Garry DJ, Richardson JA, et al. (2006) Alpha-lipoic acid prevents lipotoxic cardiomyopathy in acyl CoA-synthase transgenic mice. Biochem Biophys Res Commun 344: 446-452.

12. Zhou YT, Grayburn P, Karim A, Shimabukuro M, Higa M, et al. (2000) Lipotoxic heart disease in obese rats: implications for human obesity. Proc Natl Acad Sci USA 97: 1784-1789.

13. Boudina S, Sena S, Theobald H, Sheng X, Wright JJ, et al. (2007) Mitochondrial energetics in the heart in obesity-related diabetes: direct evidence for increased uncoupled respiration and activation of uncoupling proteins. Diabetes 56: 2457-2466.

14. Lakshmanan AP, Harima M, Suzuki K, Soetikno V, Nagata M, et al. (2013) The hyperglycemia stimulated myocardial endoplasmic reticulum (ER) stress contributes to diabetic cardiomyopathy in the transgenic non-obese type 2 diabetic rats: a differential role of unfolded protein response (UPR) signaling proteins. Int J Biochem Cell Biol 45: 438-447.

15. Lashin OM, Szweda PA, Szweda LI, Romani AM (2006) Decreased complex II respiration and HNE-modified SDH subunit in diabetic heart. Free Radic Biol Med 40: 886-896.

16. Fauconnier J, Lanner JT, Zhang SJ, Tavi P, Bruton JD, et al. (2005) Insulin and inositol 1,4,5-trisphosphate trigger abnormal cytosolic Ca2+ transients and reveal mitochondrial Ca^{2+} handling defects in cardiomyocytes of ob/ob mice. Diabetes 54: 2375-2381.

17. Pereira L, Matthes J, Schuster I, Valdivia HH, Herzig S, et al. (2006) Mechanisms of $[Ca^{2+}]i$ transient decrease in cardiomyopathy of db/db type 2 diabetic mice. Diabetes 55: 608-615.

18. Shimizu M, Umeda K, Sugihara N, Yoshio H, Ino H, et al. (1993) Collagen remodelling in myocardia of patients with diabetes. J Clin Pathol 46: 32-36.

19. Westermann D, Rutschow S, Jager S, Linderer A, Anker S, et al. (2007) Contributions of inflammation and cardiac matrix metalloproteinase activity to cardiac failure in diabetic cardiomyopathy: the role of angiotensin type 1 receptor antagonism. Diabetes 56: 641-646.

20. Bugger H, Abel ED (2009) Rodent models of diabetic cardiomyopathy. Dis Model Mech 2: 454-466.

21. Moon BC, Friedman JM (1997) The molecular basis of the obese mutation in ob2J mice. Genomics 42: 152-156.

22. Zhang Y, Proenca R, Maffei M, Barone M, Leopold L, et al. (1994) Positional cloning of the mouse obese gene and its human homologue. Nature 372: 425-432.

23. Christoffersen C, Bollano E, Lindegaard ML, Bartels ED, Goetze JP, et al. (2003) Cardiac lipid accumulation associated with diastolic dysfunction in obese mice. Endocrinology 144: 3483-3490.

24. Bartels ED, Nielsen JM, Bisgaard LS, Goetze JP, Nielsen LB (2010) Decreased expression of natriuretic peptides associated with lipid accumulation in cardiac ventricle of obese mice. Endocrinology 151: 5218-5225.

25. Semeniuk LM, Kryski AJ, Severson DL (2002) Echocardiographic assessment of cardiac function in diabetic db/db and transgenic db/db-hGLUT4 mice. Am J Physiol Heart Circ Physiol 283: H976-H982.

26. Ramirez E, Klett-Mingo M, Ares-Carrasco S, Picatoste B, Ferrarini A, et al. (2013) Eplerenone attenuated cardiac steatosis, apoptosis and diastolic dysfunction in experimental type-II diabetes. Cardiovasc Diabetol 12: 172.

27. Daniels A, Linz D, van Bilsen M, Rütten H, Sadowski T, et al. (2012) Long-term severe diabetes only leads to mild cardiac diastolic dysfunction in Zucker diabetic fatty rats. Eur J Heart Fail 14: 193-201.

28. Peterson RG, Jackson CV, Zimmerman K, de Winter W, Huebert N, et al. (2015) Characterization of the ZDSD Rat: A Translational Model for the Study of Metabolic Syndrome and Type 2 Diabetes. J Diabetes Res 487816.

29. Peterson RG, Jackson CV, Zimmerman KM (2017) The ZDSD rat: a novel model of diabetic nephropathy. Am J Transl Res 9: 4236-4249.

30. Davidson EP, Coppey LJ, Holmes A, Lupachyk S, Dake BL, et al. (2014) Characterization of diabetic neuropathy in the Zucker diabetic Sprague-Dawley rat: a new animal model for type 2 diabetes. J Diabetes Res 714273.

31. Suckow MA, Gobbett TA, Peterson RG (2017) Wound Healing Delay in the ZDSD Rat. In Vivo 31: 55-60.

32. Morgan EE, Casabianca AB, Khouri SJ, Kalinoski AL (2014) *In vivo* assessment of arterial stiffness in the isoflurane anesthetized spontaneously hypertensive rat. Cardiovasc Ultrasound 12: 37.

33. Cosson E, Valensi P, Laude D, Mesangeau D, Dabire H (2009) Arterial stiffness and the autonomic nervous system during the development of Zucker diabetic fatty rats. Diabetes Metab 35: 364-370.

34. Devereux RB, Pickering TG, Alderman MH, Chien S, Borer JS, et al. (1987) Left ventricular hypertrophy in hypertension. Prevalence and relationship to pathophysiologic variables. Hypertension 9: II53-II60.

35. Feijoo-Bandin S, Portoles M, Rosello-Lleti E, Rivera M, Gonzalez-Juanatey JR, et al. (2015) 20 years of leptin: Role of leptin in cardiomyocyte physiology and physiopathology. Life Sci 140: 10-18.

36. Minhas KM, Khan SA, Raju SV, Phan AC, Gonzalez DR, et al. (2005) Leptin repletion restores depressed {beta}-adrenergic contractility in ob/ob mice independently of cardiac hypertrophy. J Physiol 565: 463-474.

37. Purdham DM, Rajapurohitam V, Zeidan A, Huang C, Gross GJ, et al. (2008) A neutralizing leptin receptor antibody mitigates hypertrophy and hemodynamic dysfunction in the postinfarcted rat heart. Am J Physiol Heart Circ Physiol 295: H441-H446.

38. Baynes J, Murray DB (2009) Cardiac and renal function are progressively impaired with aging in Zucker diabetic fatty type II diabetic rats. Oxid Med Cell Longev 2: 328-334.

39. Krenning BJ, Geleijnse ML, Poldermans D, Roelandt JR (2004) Methodological analysis of diagnostic dobutamine stress echocardiography studies. Echocardiography 21: 725-736.

40. Pellikka PA, Roger VL, Oh JK, Miller FA, Seward JB, et al. (1995) Stress echocardiography. Part II. Dobutamine stress echocardiography: techniques, implementation, clinical applications, and correlations. Mayo Clin Proc 70: 16-27.

41. Leite S, Oliveira-Pinto J, Tavares-Silva M, Abdellatif M, Fontoura D, et al. (2015) Echocardiography and invasive hemodynamics during stress testing for diagnosis of heart failure with preserved ejection fraction: an experimental study. Am J Physiol Heart Circ Physiol 308: H1556-H1563.

42. Plante E, Lachance D, Drolet MC, Roussel E, Couet J, et al. (2005) Dobutamine stress echocardiography in healthy adult male rats. Cardiovasc Ultrasound 3: 34.

43. Rocha VZ, Libby P (2009) Obesity, inflammation, and atherosclerosis. Nat Rev Cardiol 6: 399-409.

44. Artham SM, Lavie CJ, Milani RV, Ventura HO (2009) Obesity and hypertension, heart failure, and coronary heart disease-risk factor, paradox, and recommendations for weight loss. Ochsner J 9: 124-132.

45. Ciccone M, Scicchitano P, Cameli M, Cecere A, Cortese F, et al. (2014) Endothelial Function in Pre-diabetes, Diabetes and Diabetic Cardiomyopathy: A Review. J Diabetes Metab 5: 10.

46. Zadelaar S, Kleemann R, Verschuren L, de Vries-Van der Weij J, van der Hoorn J, et al. (2007) Mouse models for atherosclerosis and pharmaceutical modifiers. Arterioscler Thromb Vasc Biol 27: 1706-1721.

47. Fredersdorf S, Thumann C, Ulucan C, Griese DP, Luchner A, et al. (2004) Myocardial hypertrophy and enhanced left ventricular contractility in Zucker diabetic fatty rats. Cardiovasc Pathol 13: 11-19.